

Scientific paper

# Probing the Temperature Unfolding of a Variety of DNA Secondary Structures Using the Fluorescence Properties of 2-aminopurine

Hui-Ting Lee,<sup>1</sup> Lela Waters,<sup>1</sup> Chris M. Olsen,<sup>1</sup> Irine Khutsishvili<sup>1</sup>  
and Luis A. Marky<sup>1,2,3,\*</sup>

<sup>1</sup> Departments of Pharmaceutical Sciences, University of Nebraska Medical Center,  
986025 Nebraska Medical Center, Omaha, NE 68198-6025

<sup>2</sup> Biochemistry and Molecular Biology, University of Nebraska Medical Center,  
986025 Nebraska Medical Center, Omaha, NE 68198-6025

<sup>3</sup> Eppley Institute for Cancer Research, University of Nebraska Medical Center,  
986025 Nebraska Medical Center, Omaha, NE 68198-6025

\* Corresponding author: E-mail: lmarky@unmc.edu  
Tel: (402) 559-4628; Fax: (402) 559-9543; E-mail:

Received: 14-03-2012

Dedicated to Prof. Dr. Gorazd Vesnaver on the occasion of his 70<sup>th</sup> birthday

## Abstract

The fluorescence probe 2-aminopurine (2AP) is widely used to monitor the molecular environment, including the local solvent environment, and overall dynamics of nucleic acids and nucleic acid-ligand complexes. This work reports on the temperature-induced conformational flexibility of a variety of secondary structures of nucleic acids using optical and calorimetric melting techniques, and evaluates the usefulness of fluorescence melting curves obtained from monitoring the fluorescence changes of 2AP as a function of temperature. Furthermore, the base stacking properties of 2AP are examined in these structures for a first time. Specifically, we incorporated single A → 2AP substitutions into a variety of DNA structures, such as a single strand (SS), a dodecamer duplex (Duplex), a hairpin loop (Hairpin), a G-quadruplex (G2), and an intramolecular triplex (Triplex). A combination of fluorescence, UV, and circular dichroism spectroscopies, and differential scanning calorimetric (DSC) techniques is used to investigate their temperature-induced unfolding. The melting curves of each molecule show monophasic transitions with similar  $T_M$ s and van't Hoff enthalpies indicating that all transitions are two-state and that the fluorescence changes for the unstacking of 2AP follow the unfolding of the whole molecule. The DSC thermodynamic profiles of each 2AP modified molecule, relative to their unmodified control molecules, yielded folding  $\Delta\Delta G^\circ$ s of 1.6 kcal/mol (Duplex), 3.1 kcal/mol (Hairpin), 1.6 kcal/mol (Triplex), and -1.7 kcal/mol (G2). These  $\Delta\Delta G^\circ$ s are driven by unfavorable differential enthalpies (Duplex and Hairpin), favorable differential enthalpy (G2), and by a favorable differential entropy term for Triplex. These enthalpy effects are explained in terms of stacking and hydration contributions, that are associated with the local environment that 2AP is experiencing. For example, the lower  $\Delta\Delta H_{\text{cal}}$  value of 8.7 kcal/mol (Hairpin), relative to Duplex, is due to weaker base-pair stacks and higher hydration state of the stem of Hairpin. We conclude that the incorporation of 2AP in nucleic acids is a useful tool to monitor their temperature-induced unfolding; especially, when these sensitive fluorescent moieties are placed in the proper molecular environment of the nucleic acid.

**Keywords:** 2-Aminopurine, Fluorescence, 2AminoPurine•T base-pair stacking, Differential Scanning Calorimetry, Unfolding thermodynamics,

## 1. Introduction

Nucleic acids function as carriers of information and directors of cell activity upon interaction with pro-

teins and other ligands. The molecular interactions stabilizing these nucleic acid-ligand complexes depend on the structure and stability of both the nucleic acid and of the particular ligand. Therefore, to understand how nuc-

leic acids carry out their roles in the cell, it is necessary to determine their conformations and overall physical properties. The stability of a nucleic acid molecule depends globally on the extent of base pairing and base pair stacking, as well as ion and water interactions. Fluorescence techniques have been used to study the physical properties of DNA.<sup>1–5</sup> Due to a low quantum yield and fast lifetime, the intrinsic fluorescence of DNA is very weak; however, a synthetic fluorescent base can be substituted for a canonical base in a DNA molecule.<sup>1</sup> The best example of a fluorescent base is 2-aminopurine (2AP). 2AP is a fluorescent analog of the purine bases with its amino group in the 2 position rather than 6 as in adenine (Figure 1a).<sup>6</sup> 2AP has been previously incorporated into DNA to substitute for adenine or guanine, forming two and one hydrogen bond(s) when paired with thymine and cytosine,<sup>7–9</sup> respectively (Figure 1b). The absorption maximum of 2AP occurs at longer wavelengths (~ 305 nm) than those of the purine and pyrimidine bases so it can be selectively excited even in the presence of a large excess of other bases.<sup>2,6,10</sup> The fluorescence quantum yield, lifetime and intensity decay kinetics of the incorporated 2AP in nucleic acids are affected by aromatic stacking, collisional interactions with neighboring bases and local hydration environment.<sup>10–13</sup> These properties make 2AP an ideal probe to follow the temperature-induced conformational transitions of DNA. Furthermore, 2AP has been used widely as a probe to investigate the local environment of nucleic acids with different base modifications, including the effects of mismatches,<sup>9,14</sup> abasic sites,<sup>15</sup> dynamics of RNA hairpin loops,<sup>16</sup> structural dynamics of DNA,<sup>3,7,17–19</sup> RNA<sup>20–21</sup> and DNA/RNA hybrids,<sup>11</sup> nucleic acid-protein<sup>22–23</sup> and nucleic acid-ligand interactions.<sup>24</sup> In general, the fluorescence properties of 2AP depend on the lo-

cal environment that it experiences, including the effects of the solvent. And, its fluorescence intensity changes as a DNA molecule undergoes a temperature-induced conformational transition from the native state to the random coil state. However, the base stacking contributions and overall thermodynamic stability of 2AP, when placed in nucleic acids, has not been investigated previously. The significance of this manuscript is that we correlate temperature-unfolding profiles obtained from a variety of optical and calorimetric techniques to examine the usefulness of 2AP to monitor the temperature-induced conformational flexibility of nucleic acids, and to measure its stability and stacking contributions.

In this work, we report on the temperature-induced unfolding of DNA oligonucleotides forming different secondary structures, such as a single strand, duplex, hairpin loop, quadruplex and triplex motifs. Each structure has single 2AP incorporated more or less at the center of the molecule. Their fluorescence melting curves were obtained and compared with their UV, CD and DSC melting curves. The results show that all four techniques produce melting curves with similar shapes i.e., similar transition temperatures and van't Hoff enthalpies. The combined results indicate that the 2AP fluorescence changes are monitoring the global unfolding of the molecule. Furthermore, the comparison of the DSC thermodynamic profiles, with and without 2AP, shows that the single placement of 2AP destabilizes duplex, hairpin loop and triplex structures, but it stabilizes the G-quadruplex. Overall, the destabilizing effect for the placement of a 2AP•dT base pair between two dA•dT base pairs is due to lower stacking contributions, while the stabilizing effect of the TXT loop of the G-quadruplex is due to additional stacking contributions of this loop with the G-quartet at the top of this molecule.

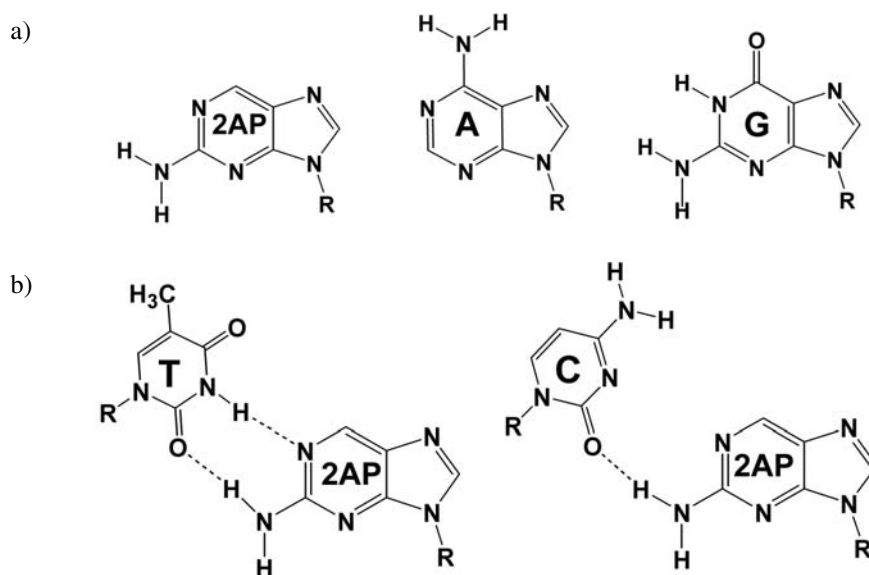


**Figure 1.** (a) Structures of 2-aminopurine monomer (2AP) and purine bases. (b) Base-pairing scheme of 2AP with thymine or cytosine.

## 2. Materials and Methods

### 2. 1. Materials

The 2AP-modified oligodeoxynucleotides, shown in Figure 2, and unmodified oligonucleotides were synthesized by the Eppley Institute Molecular Biology Core facility at UNMC, purified by reverse-phase HPLC, desalted on a G-10 Sephadex column, and lyophilized to dryness. The 2AP phosphoramidite was obtained from Glen research (Sterling, VA), and the procedures recommended by this supplier were used in the synthesis of each oligonucleotide. The concentration of each oligonucleotide was determined spectrophotometrically at 260 nm and 90 °C using the following molar extinction coefficients for the 2-aminopurine modified oligonucleotides, in  $\text{mM}^{-1} \text{cm}^{-1}$ : 110 (*SS*, 111), 112 (*Duplex*, 112), 144 (*Hairpin*, 144), 268 (*Triplex*, 271) and 148 (*G2*, 147), the numbers in parenthesis correspond to the unmodified oligonucleotides. The experiments were conducted using the following buffers: 10 mM sodium phosphate, 0.1 or 0.2 M sodium chloride at pH 7 (*SS*, *Duplex*, *Hairpin* and *Triplex*), and 10 mM Cs-Hepes, 100 mM KCl at pH 7.5 (*G2*). The *G2* unmodified and control molecule used in this work corresponds to the G-quadruplex with a TAT top loop rather than the conventional G2 or thrombin aptamer with the TGT loop.<sup>25–27</sup>

obtained by following the changes in the intensity of the fluorescence emission at 370 nm from 5 °C to 100 °C, using a heating rate of  $\sim 0.7$  °C/min, and oligonucleotide concentrations of  $\sim 4.2$   $\mu\text{M}$  with the exception of *Triplex* that 2.2  $\mu\text{M}$  was used. The cell compartment was flushed with nitrogen to prevent water condensation at temperatures below room temperature.

**Temperature-Dependent UV and Circular Dichroism (CD) Spectroscopies.** Absorbances versus temperature profiles (UV melting curves) were obtained at 297 nm for G2, and at 260 nm for all other molecules, using a thermoelectrically controlled Aviv 14DS spectrophotometer (Lakewood, NJ). The temperature was scanned from 5 °C to 95 °C at a heating rate of  $\sim 0.5$  °C/min. The CD spectra of each oligonucleotide, from 200 nm to 350 nm, were obtained at several temperatures using an Aviv Model-202SF spectrometer (Lakewood, NJ), equipped with a peltier system for temperature control. This allowed us to determine the conformation of each oligonucleotide, from simple inspection of their CD spectra at low temperatures, and to select appropriate wavelengths for their temperature-induced unfolding. Ellipticities versus temperature profiles (CD melting curves) were obtained at 275 nm for G2 and 250 nm for all the other molecules. The temperature

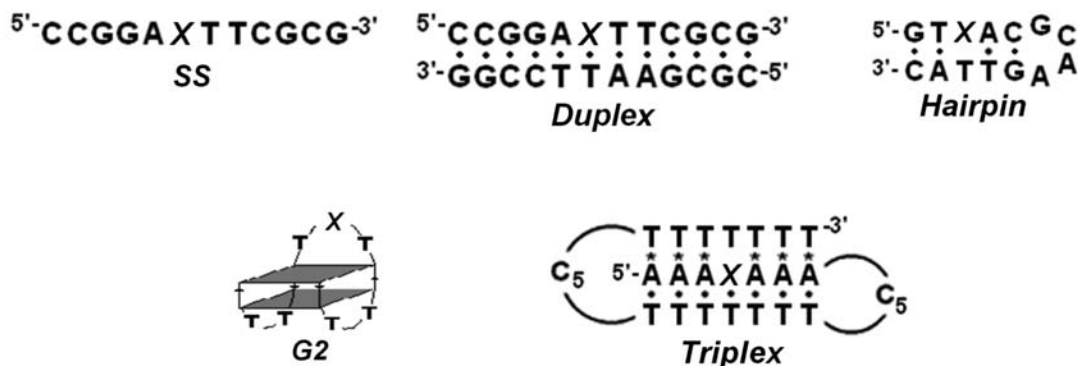


**Figure 2.** Sequences, structures and designation of the oligonucleotides investigated, X stands for 2-aminopurine in all of the modified molecules and replaces adenine in the control molecules.

### Temperature-Dependent Fluorescence Spectroscopy.

The fluorescence measurements were obtained using an AVIV Model-ATP105 spectrofluorometer (Lakewood, NJ), or a Varian Cary Eclipse Fluorescence spectrophotometer (Walnut Creek, CA), each equipped with a peltier system for temperature control. The fluorescence emission spectra of the modified oligonucleotides were obtained from 300 nm to 400 nm at several temperatures, using an excitation wavelength of 307 nm, the emission and excitation slits were set at 5 nm. A similar fluorescence emission spectrum for *Triplex* was obtained using both instruments, allowing us to select the wavelength of maximum fluorescence emission for the temperature-induced unfolding studies. Fluorescent (FL) melting curves were

was scanned from 5 °C to 95 °C at a heating rate of  $\sim 0.7$  °C/min, and the cell compartment was flushed with nitrogen to prevent water condensation.

**Analysis of the Optical Melting Curves.** To compare the shape of all three optical melting curves, each experimental melting curve was converted to an “ $\alpha$ ” curve using standard procedures i.e., the extent of the unfolding reaction is plotted as a function of temperature.<sup>28</sup> In this procedure,  $\alpha$  is defined as the fraction of strands in the folded state, and is calculated by the level rule at several temperatures throughout the experimental curve i.e.,  $\alpha$  is equal to the distance between the high-temperature baseline and the experimental curve divided by the distance between the low and high

temperature baselines.<sup>28</sup> This van't Hoff analysis of the shape of each melting curve yielded  $T_M$ s and  $\Delta H_{vH}$ s as shown previously.<sup>28</sup> Furthermore, the transition molecularity for the unfolding of a particular secondary structure was determined from the  $T_M$ -dependence on strand concentration. The  $T_M$  of intramolecular complexes does not depend on strand concentration while the  $T_M$  of intermolecular complexes does depend on concentration.<sup>29,30</sup>

**Differential Scanning Calorimetry (DSC).** The total heat required for the unfolding of each oligonucleotide was measured with a VP-DSC differential scanning calorimeter from Microcal (Northampton, MA). Standard thermodynamic profiles are obtained from a DSC experiment using the following relationships:  $\Delta H_{cal} = \int \Delta C_p(T) dT$ ;  $\Delta S_{cal} = \int \Delta C_p(T)/T dT$ , and the Gibbs equation,  $\Delta G^\circ_{(T)} = \Delta H_{cal} - T\Delta S_{cal}$ ; where  $\Delta C_p$  is the anomalous heat capacity of the oligonucleotide solution during the unfolding process,  $\Delta H_{cal}$  is the unfolding enthalpy, and  $\Delta S_{cal}$  is the unfolding entropy. Both latter terms are temperature-dependent i.e., the heat capacity difference between the initial and final states is non-zero. Alternatively,  $\Delta G^\circ_{(T)}$  can be calculated using the equation  $\Delta G^\circ_{(T)} = \Delta H_{cal} (1 - T/T_M)$  which is implicitly correct for the unfolding of intramolecular complexes. The  $\Delta H_{vH}$  terms are also obtained from the DSC profiles using the temperatures at the half-width height of the experimental curve.<sup>28</sup> The  $\Delta H_{vH} / \Delta H_{cal}$  ratio can tell us about the nature of the transition, for a two-state transition  $\Delta H_{vH} = \Delta H_{cal}$ , while for a non-two-state  $\Delta H_{vH} \neq \Delta H_{cal}$  (28,29). Furthermore, the differential curves obtained in these DSC experiments were converted to integral curves by stepwise integration of the experimental curves as a function of temperature every 0.2 °C throughout the transition. This procedure yields  $\Delta H_{cal}$  versus T curves that are similar in shape to the “ $\alpha$ ” curves; therefore, these curves are also included in the comparison of the “ $\alpha$ ” curves obtained from FL, UV and CD melting experiments.

### 3. Results and Discussion

#### 3.1. Design of Molecules

The sequences, structures and designations of all molecules are shown in Figure 2. The X denotes the base substitution sites of 2AP for adenine. The 1:1 mixture of non-self-complementary single strand d(CCGGAXTTCGCG), *SS*, and its complement d(CGCGAATTCGG) yielded a non-self-complementary duplex, *Duplex*. The sequences d(GTXACGCAAGTTAC), d(A<sub>3</sub>XA<sub>3</sub>C5T<sub>7</sub>C<sub>5</sub>T<sub>7</sub>), and d(G<sub>2</sub>T<sub>2</sub>G<sub>2</sub>TXTG<sub>2</sub>T<sub>2</sub>G<sub>2</sub>) are designed to form a hairpin, triplex, and G-quadruplex, respectively, intramolecularly.

#### 3.2. Fluorescence Melting Curves

Initially, the changes in the intensity of fluorescence of 2AP as a function of temperature were obtained in

10 mM sodium phosphate, 200 mM NaCl, pH 7, a buffer that is used for the majority of the thermal transitions. The emission intensity of the 2AP monomer at 370 nm, using an excitation wavelength of 307 nm, decreases linearly with increasing temperature (Figure 3a), as reported earlier.<sup>6</sup> This corresponds to changes in the geometry of the 2AP excited state, and its associated hydration state, as the temperature is increased.<sup>6,18</sup> The incorporation of 2AP into a single-stranded oligonucleotide (*SS*) caused a decrease in its emission intensity at 5 °C from 0.53 (2AP) to 0.06 (*SS*), see Figure 3a. The *SS* emission intensity is 14 times less than the monomer intensity at 95 °C, decreasing from 0.24 (2AP) to 0.021 (*SS*), Figure 3a only shows this drop up to 77.5 °C. This decrease of the *SS* fluorescence intensity compared to the monomer may result from a lower exposure to the solvent and the quenching effect of the adjacent bases, i.e., in the *SS*, 2AP is stacked on the neighboring thymine and adenine bases.<sup>11,12,31</sup> Moreover, the fluorescence intensity changes between 5 °C and 95 °C for *SS* (2.8) are greater than for 2AP (2.1), an effect consistent with a lower exposure of 2AP to the solvent in *SS*. The sigmoidal shape of the *SS* curve (Figure 3a) indicates a broad unfolding with a 48% drop in the emission intensity over a 15–50 °C temperature range. The nearly linear change at high temperatures also has a downward slope, which is consistent with the reduction of 2AP fluorescence with temperature, and with all other oligonucleotides, and may be simply due to a temperature effect on the excited state of 2AP. The main observation is that this fluorescence technique is able to detect an unfolding transition of the *SS* with a  $T_M$  of 36.6 °C, which corresponds to breaking base-base stacking interactions in this single-strand. Figure 3a also shows the FL melting curve of *Duplex*, in this curve a significant reduction in the fluorescence intensity at 5 °C, to 0.02, is observed when the complementary strand is added to *SS*. This lowering is due to the formation of a duplex, corresponding to the stacking of 2AP within base-pair stacks that are known to quench the fluorescence of 2AP.<sup>2,11,12,31</sup> This implies that 2AP is experiencing the base-pair stacks environment away from the solvent. In the FL melting curve of *Duplex* (Figure 3a), there is a gradual decrease in the fluorescence intensity as the temperature is increased to ~ 40 °C, followed by an increase in the intensity, i.e., a somewhat cooperative monophasic transition with a  $T_M$  of 56.5 °C takes place. After 65 °C, the curve again declines linearly in a similar way to *SS* to an intensity value of 0.017 at 95 °C, indicating a similar environment for 2AP at high temperatures, corresponding to the random coil state of *SS*. These fluorescence changes clearly indicate the effects 2AP experiences with temperature, including exposure of 2AP to solvent and changes in the binding of ions and water molecules, clearly showing the unfolding of *Duplex*. The fluorescent melting curves of the other 2AP modified oligonucleotides are shown in Figures 3b and 3c. The fluorescence intensity of *G2* decreases with increasing tempe-

perature and shows a sharp increase of about 13% from 40 °C to 60 °C. These changes show a monophasic transition curve with  $T_M$  of 49.1 °C, as reported earlier.<sup>25</sup> This FL curve also has a fluorescence intensity of 0.01 at 95 °C, which is similar to *SS* and *Duplex*. Since 2AP is incorporated in the middle of the top loop of this G-quadruplex, its FL melting curve indicates that initially the T-2AP-T loop is stacked on top of the G-quadruplex. As the temperature is increased the loop becomes unstacked and eventually the whole oligonucleotide becomes a random coil or the whole molecule unfolds together. The FL melting curve of *Hairpin* (Figure 3b) shows a sigmoidal behavior with increasing temperature and linear baselines at low and high temperatures with negative slopes. The emission intensity increases by 9% during the transition, while the emission intensities at 5 °C and 95 °C are more or less similar to the intensities measured with the FL curves of *G2* and *Duplex*. *Hairpin* undergoes a temperature-induced unfolding transition with a  $T_M$  of 59.9 °C, i.e., the base-pair stacks in the stem of *Hairpin* are broken with temperature. However, *Hairpin* has a slightly lower fluorescence intensity at 95 °C (equal to 0.01), suggesting some residual stacking of 2AP with the neighboring adenine at the 3'-side, while thymine is the neighboring base in both *G2* and *Duplex*, see Figure 2. This small effect invokes a sequence nearest-neighbor effect in the 5' to 3' direction.<sup>15,32</sup> The smaller change in the fluorescence intensity of *Hairpin* (9%), relative to *Duplex* (23%), may be due to the small number of base-pair stacks in its helical stem, equal to 5 versus 11 in *Duplex*. Thus, the base-pair stacks of a half helical turn are somewhat flexible, and 2AP in the middle of its stem senses a relatively hydrated stem. Alternatively, the 2AP•T base pair is more exposed to the solvent or in faster exchange with the solvent. Figure 3c shows the FL melting curve of *Triplex*, this melting curve was obtained at both higher concentration and photomultiplier voltage; therefore, its emission intensities at 5 °C and 95 °C can not be compared directly with the emission intensities of the other molecules. The curve shows a true sigmoidal shape indicating the cooperative unfolding of the base-triplet stacks of this triple helical structure. The overall unfolding of *Triplex* is monophasic and is accompanied by a ~500% change in fluorescence emission intensity, and  $T_M$  of 32.7 °C. This shows that 2AP at the center of *Triplex* and flanked by two thymine bases is experiencing a less hydrophilic environment i.e. the T•2AP•T base-triplet is stacked within two T•A•T base triplets with a very effective screening of water molecules at low temperatures.

### 3. 3. Melting Behavior of Oligonucleotides Determined from Temperature-Dependent UV and CD Spectroscopies

To compare the FL melting curves with other optical methods, UV and CD melts of all the molecules were ob-

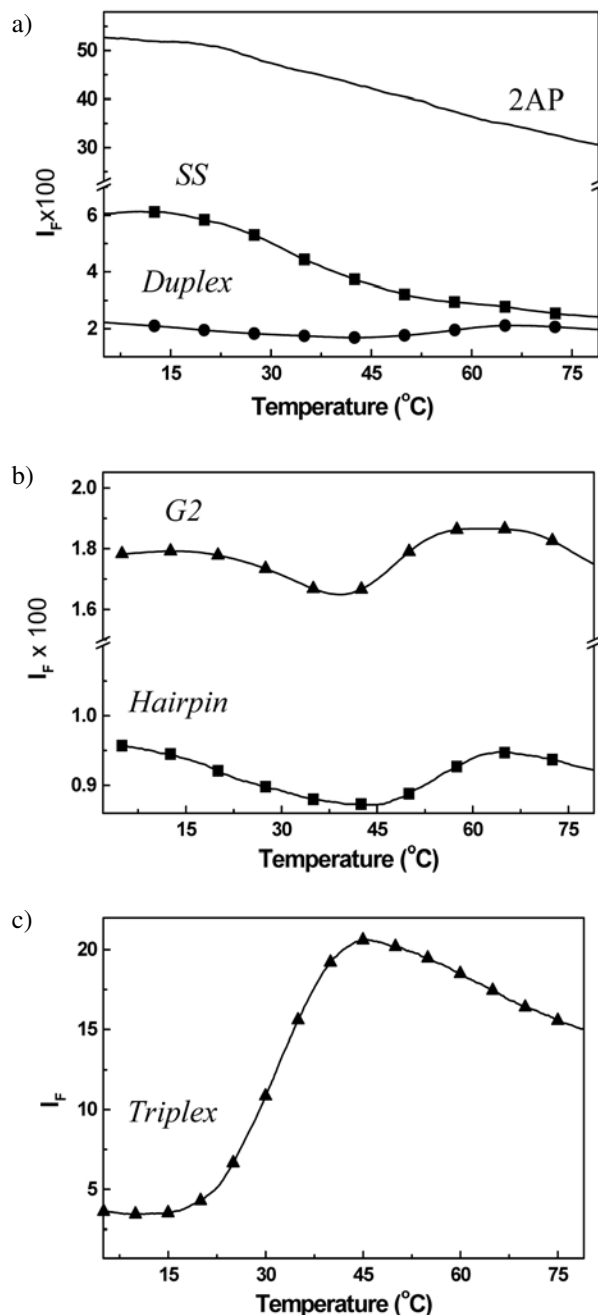


**Figure 3.** Fluorescence melting curves of 2AP monomer (solid line) and 2AP modified oligonucleotides. Please note that for clarity, the Y-axis correspond to different scales. All experiments were done in 10 mM sodium phosphate buffer, 200 mM NaCl at pH 7, except *G2*, which was done in 10 mM Cs-HEPES, 100 mM KCl, pH 7.5.

tained using the same solution conditions as in the fluorescent experiments. UV melting curves at 297 nm for *G2* and 260 nm (all other molecules) are shown in Figure 4, these wavelengths were chosen because of their larger absorbance difference between the low- and high-temperature UV spectra (data not shown). All the curves done at

260 nm show a hyperchromic effect, while *G2* shows a hypochromic effect at 297 nm. The helix-coil transition of each molecule is monophasic. The observed hyperchromicity values for these transitions are 5% (*SS*), 12.5% (*Hairpin*), 15% (*Duplex*) and 20% (*Triplex*), while a 39% hypochromicity is observed for *G2*. These UV melting curves were converted to “ $\alpha$ ” curves to obtain  $T_M$ s and  $\Delta H_{VH}$ s. The results are presented in Table 1. To check the molecularity of these secondary structures, melting curves were obtained as a function of strand concentration over a tenfold range in strand concentration (data not shown). The  $T_M$ s for each molecule remained constant indicating that all are unimolecular; the one exception is *Duplex*, its

$T_M$  increases with the increase in strand concentration, consistent with its bimolecular formation.

CD melting curves were also performed at wavelengths with the largest difference in high and low temperature ellipticities: 292 nm for *G2* and 250 nm for the other molecules (Figure 4). All CD melting curves show sigmoidal monophasic transitions and an increase in the molar ellipticity at 250 nm. While *Hairpin* did not show any changes in molar ellipticity (data not shown), *G2* actually shows a decrease in the molar ellipticity at 275 nm. The observed molar ellipticity changes for these transitions are ( $\times 10^{-6}$  deg cm<sup>2</sup> mol<sup>-1</sup>): 1.34 (*SS*), 2.28 (*Duplex*) and 1.79 (*Triplex*), while  $-0.83$  for *G2*. CD

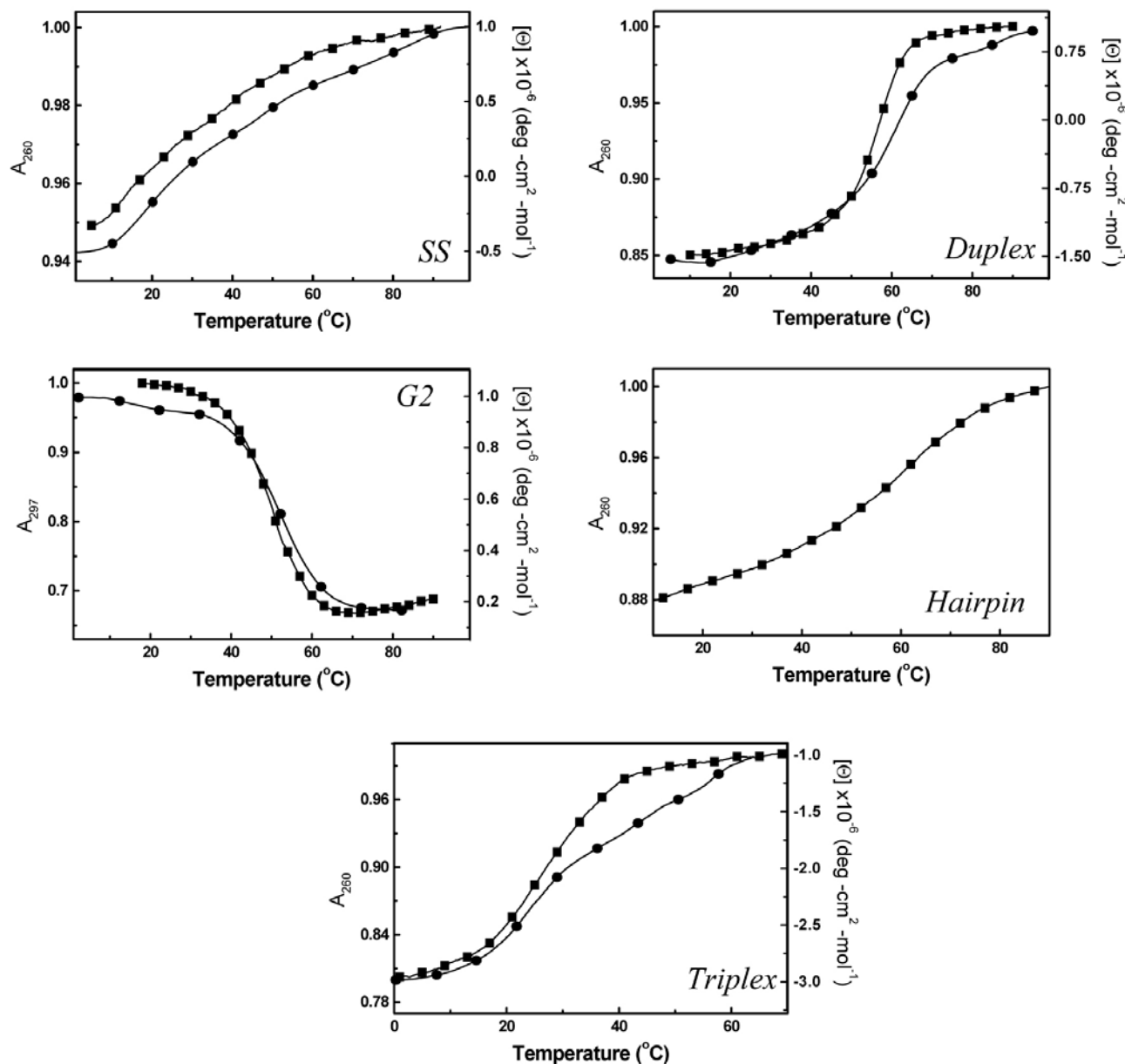


**Figure 4.** UV (squares) and CD (circles) melting curves of 2AP modified oligonucleotides. All experiments were done in 10 mM sodium phosphate buffer, 200 mM NaCl at pH 7, except *G2*, which was done in 10 mM Cs-HEPES, 100 mM KCl, pH 7.5.

**Table 1.**  $T_M$ s and van't Hoff enthalpies obtained from FL, UV, CD and DSC Melts.

DNA	FL		UV		CD		DSC	
	$T_M$ (°C)	$\Delta H_{vH}$ (kcal/mol)						
SS	36.6	25	~ 38	ND	~ 38	ND	38.0	23
Duplex	56.5	73	56.1	89	59.0	78	57.6	93
Hairpin	59.9	29	60.5	29	ND	ND	62	25
Triplex	32.7	39	31.3	36	31.5	38	31.0	41
G2	49.1	44	50.6	46	49.8	43	51.4	43

Experimental errors are as follows:  $T_M$  ( $\pm 0.5$  °C),  $\Delta H_{vH}$  ( $\pm 15\%$ ).

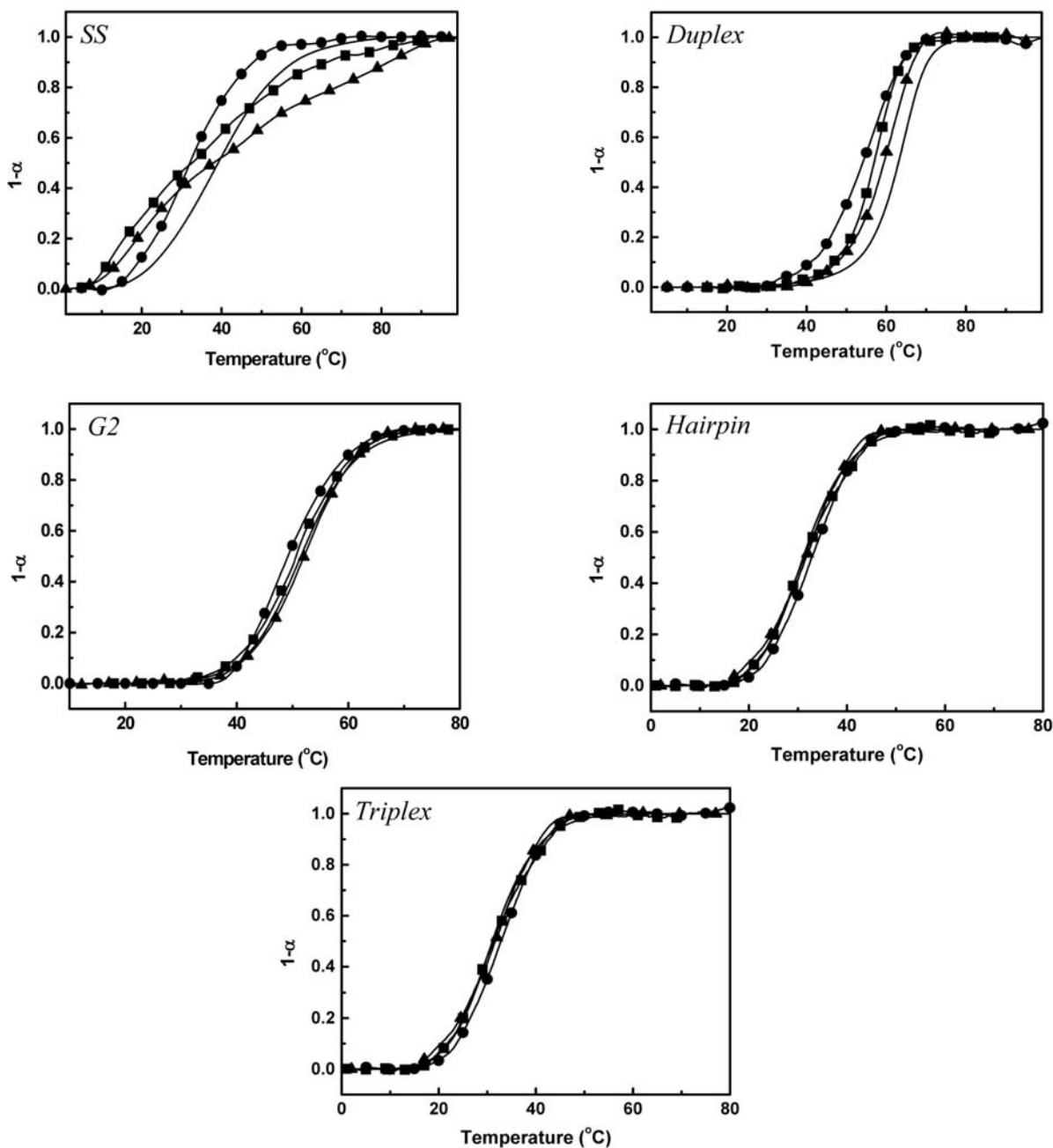


**Figure 5.** The “ $\alpha$ ” curves obtained from fluorescence (circles), UV (squares), CD (triangles) and DSC (solid line) melting curves of 2AP modified molecules.

melting curves were converted to “ $\alpha$ ” curves to obtain  $T_{M,S}$  and  $\Delta H_{vH,S}$  from analysis of their shape. The results as presented in Table 1 are discussed in the following section.

### 3. 4. Shape Analysis of FL, UV, CD and DSC Melting Curves

We hypothesize that the FL signal of 2AP reports on the local melting of the base-pair stacks and that the temperature-induced transition experienced by 2AP provides accurate information on the state of folding of the entire molecule. To test this hypothesis, FL melting curves are compared with those obtained using a variety of experimental observables, such as UV absorbance, ellipticity and heat capacity. This is done by comparing the shape of the four types of melting curves for the unfolding of a given molecule i.e., comparing their  $T_{M,S}$  and  $\Delta H_{vH,S}$  parameters. The transitions observed in each type of melting curve and for all molecules were converted to “ $\alpha$ ” curves by a procedure outline elsewhere.<sup>28</sup> These “ $\alpha$ ” curves are shown in Figures 5. The resulting  $T_{M,S}$  and  $\Delta H_{vH,S}$  determined from van't Hoff analysis of the shape of each melting curve are presented in Table 1. In summary, we obtained  $T_{M,S}$  and  $\Delta H_{vH,S}$  in the following ranges, respectively: 36.6–38.0 °C and 23–25 kcal/mol (*SS*), 56.1–59.0 °C and 73–93 kcal/mol (*Duplex*), 59.9–62.0 °C and 25–29 kcal/mol (*Hairpin*), 31.1–32.7 °C and 36–41 kcal/mol (*Triplex*), 49.1–51.4 °C and 43–46 kcal/mol (*G2*). Considering the experimental errors in the determination of the  $T_M$  ( $\pm 0.5$  to  $\pm 1$  °C, depending on the technique used) and  $\Delta H_{vH}$  (15%), the agreement in these parameters is excellent for the majority of the molecules. This comparison shows that all four types of experiments monitor the unfolding of the whole molecule. The similarities in the  $\Delta H_{vH}$  values for their unfolding not only indicates that their shapes are similar, but also shows that their transition is two-state. This two-state melting behavior of each molecule is the main reason that the FL melting curve is monitoring the unfolding of the whole molecule. We conclude that the proper placement of 2AP is an important criterion to consider in the temperature-induced unfolding of a nucleic acid molecule.

**Base Pair Stacking Contributions of 2AP.** We used differential scanning calorimetry to determine if 2AP alters base-pair stacking interactions when incorporated into various types of nucleic acid structures. DSC experiments of the 2AP modified molecules and their unmodified control molecules were performed using similar solution conditions. Typical DSC unfolding curves for each nucleic acid secondary structure are shown in Figure 6. The unfolding of each molecule undergoes highly reproducible monophasic transitions. Furthermore, the initial and final states of each have similar heat capacity values, which indicate that their unfolding is accompanied by negligible heat ca-

capacity effects. The  $T_{M,S}$  obtained from the DSC melts (Table 2) for the unmodified molecules are similar to those obtained from UV and CD melts, in spite of different strand concentrations, and consistent with their intramolecular formation. However, the unmodified *SS* shows a broad transition with a slightly higher  $T_M$  than the one obtained in the FL melt. This transition is very broad and is not seen in the UV and CD melts, and may correspond to the unfolding of a weak intramolecular hairpin structure or to simply breaking base-base stacking interactions in this strand. Furthermore, the higher  $T_M$  of *Duplex* obtained from DSC is due to its bimolecular formation and the higher concentrations used in DSC.<sup>28</sup> The complete thermodynamic profiles for the folding of each secondary structure at 5 °C are shown in Table 2. The favorable  $\Delta G^\circ_{(5)}$  for the formation of each molecule results from the characteristic compensation of a favorable enthalpy term with an unfavorable entropy contribution. The favorable enthalpy terms are due primarily to stacking contributions. Base-pairing contributions are normally small, the immobilization of electrostricted water, if any, and the putative removal of structural water may also contribute with exothermic heats. The unfavorable entropy contribution is mainly due to the ordering of a random coil into the particular secondary structure, uptake of ions and water molecules. The nature of each transition for the unmodified molecules was analyzed by simple inspection of the  $\Delta H_{vH}/\Delta H_{cal}$  ratio, the average  $\Delta H_{vH}$  values of the FL, UV, CD, and DSC melting curves is used in this ratio. We obtained an  $\Delta H_{vH}/\Delta H_{cal}$  ratio of 0.5 for *Triplex*, a result consistent with previous reports on the non two-state unfolding behavior of this type of intramolecular triplex.<sup>33–35</sup> The other molecules have  $\Delta H_{vH}/\Delta H_{cal}$  ratios of  $1.14 \pm 0.2$ , that indicate these molecules unfold in a two-state fashion, i.e. no intermediate states are present. In terms of thermal stability, the A  $\rightarrow$  2AP (or A•T  $\rightarrow$  2AP•T) substitution in each molecule shifts the  $T_M$  to lower temperatures, for *Duplex* (by 4.7 °C), *Hairpin* (by 8.1 °C), and *Triplex* (6.6 °C), but shifts the  $T_M$  of *G2* to higher temperatures (by 6.1 °C); moreover, lower unfolding enthalpies are obtained for all molecules, the exception is the modified *G2* that yielded a larger unfolding enthalpy. To determine the stacking contributions for the incorporation of 2AP, the folding enthalpies (Table 2) of the 2AP modified molecules are subtracted from those of the control molecules, this exercise yields  $\Delta\Delta H_{cal,S}$  of 5.9 kcal/mol (*Duplex*), 14.6 kcal/mol (*Hairpin*), 0.3 kcal/mol (*Triplex*) and –4.0 kcal/mol (*G2*). The magnitude of these differential enthalpy terms indicate that the A  $\rightarrow$  2AP substitutions decrease stacking contributions to the stability of *Duplex* and *Hairpin* but have no effect on *Triplex*. The substitution increases stacking contributions to the stability of *G2*. The overall effects can be explained in terms of the placement of 2AP in these molecules together with its degree of solvent exposure and overall hydration state (observed in the FL melting curves). For instance, the much lower

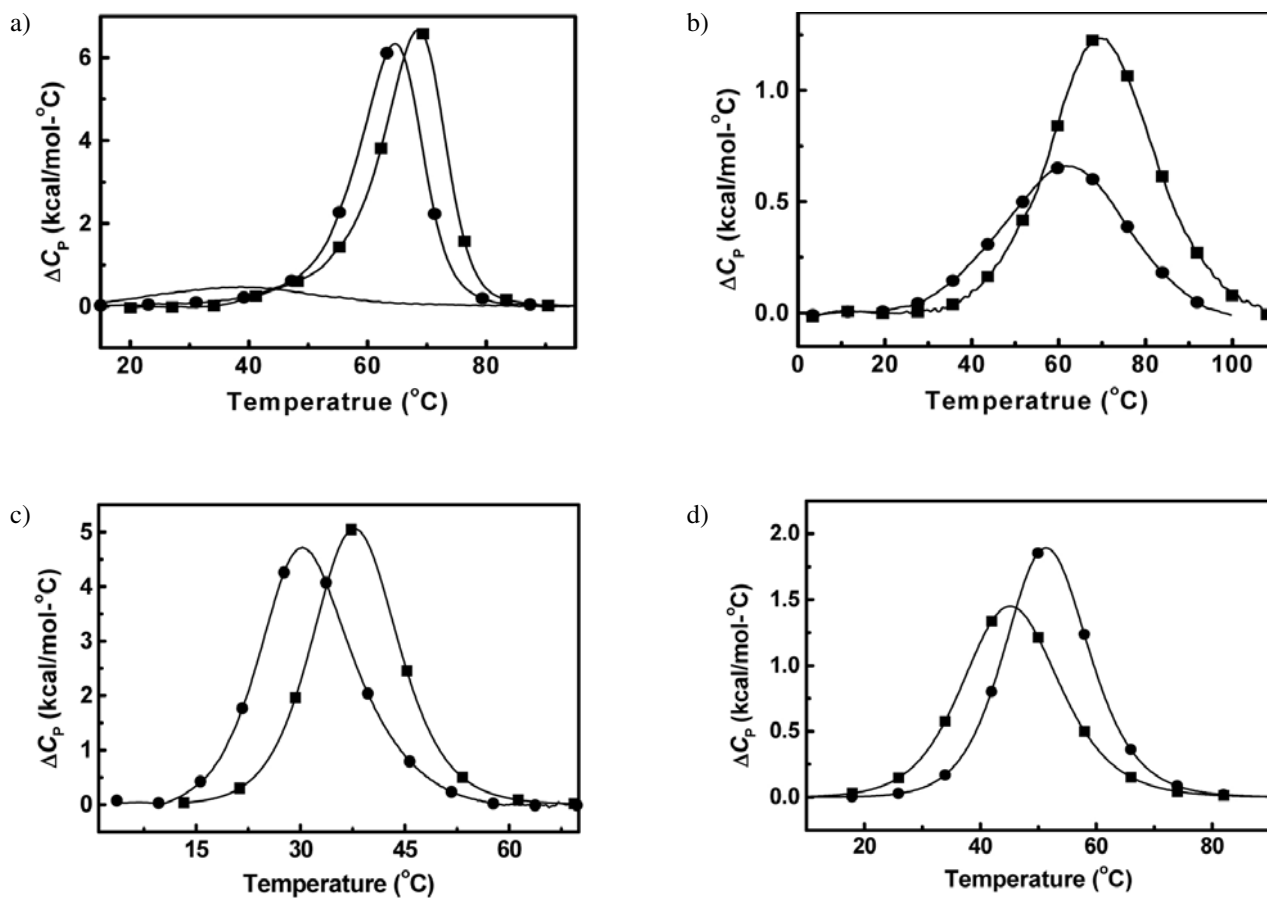


**Figure 6.** DSC melting curves of all 2AP modified (circles) and control (squares) molecules: (a) *Duplex* and *SS* (line), (b) *Hairpin*, (c) *Triplex* and (d) *G2*. All experiments were done in 10 mM sodium phosphate buffer, 200 mM NaCl at pH 7, except *G2*, which was done in 10 mM Cs-HEPES, 100 mM KCl, pH 7.5.

$\Delta\Delta H_{\text{cal}}$  value of *Hairpin*, and relative to *Duplex*, by 8.7 kcal/mol, is due to weaker base-pair stacks and higher hydration state of the double helical stem of *Hairpin*. The modified *Triplex* has similar strength of base-triplet stacks and similar overall hydration state than the control triplex molecule. In the modified *G2*, the T-2AP-T loop is well stacked on top of the G-quadruplex, which has a lower hydration state than any of the other secondary structures investigated.<sup>25,36</sup> In terms of the thermodynamic stability, we obtained folding  $\Delta\Delta G^{\circ}_{(5)}$  terms (Table 6.2) of 1.6 kcal/mol (*Duplex*), 3.1 kcal/mol (*Hairpin*), 1.6 kcal (*Triplex*), and  $-1.7$  (*G2*), which are driven by unfavorable differential enthalpies (*Duplex* and *Hairpin*), favorable differential enthalpy (*G2*) and by a favorable differential entropy term for *Triplex*. Overall, the presence of 2AP has a destabilizing effect, with the exception of *G2*,<sup>25</sup> which is consistent with previous reports.<sup>9,14</sup> However, *Triplex* is less perturbed with a similar differential enthalpy, indicating that the T•2AP•T base triplet stacks well within the adjacent T•A•T base triplets and the thymine flanking of 2AP is effectively burying 2AP from the solvent.

## 4. Conclusions

We used a combination of temperature-dependent fluorescence, UV, circular dichroism spectroscopies to thermodynamically characterize the melting behavior of five DNA structures: a single strand, an intermolecular duplex, a hairpin loop, a triplex and a G-quadruplex. Standard thermodynamic profiles, including van't Hoff enthalpies obtained from the different techniques, were obtained for their unfolding to random coil states. All melting curves for each molecule show monophasic transitions with similar  $T_M$ s, and van't Hoff enthalpies, indicating that all transitions are two-state and that the fluorescence changes for the unstacking of 2AP follow the unfolding of the whole molecule. The comparison of the DSC thermodynamic profiles of each 2AP modified molecule, and relative to their unmodified control molecules, shows that the single placement of 2AP yielded unfavorable folding differential free energies (*Duplex*, *Hairpin* and *Triplex*), and a favorable folding differential free energies for *G2*, which are driven by unfavorable differential enthalpies (*Duplex* and *Hairpin*), favorable differential enthalpy

**Table 2.** Thermodynamic profiles for the folding of nucleic acid structures.<sup>a</sup>

DNA	$T_M$ (°C)	$\Delta H_{cal}$ (kcal/mol)	$T\Delta S_{cal}$ (kcal/mol)	$\Delta G^{(s)}$ (kcal/mol)
<i>SS</i>				
Modified	38.0	-17.6	-15.6	-2.0
<i>Duplex</i>				
Modified	57.6	-95.1	-80.0	-15.7
Control	62.3	-101	-83.7	-17.3
<i>Hairpin</i>				
Modified	62.0	-24.8	-20.6	-4.2
Control	70.1	-39.4	-31.8	-7.3
<i>Triplex</i>				
Modified	31.0	-82.8	-75.7	-7.1
Control	37.6	-82.5	-73.8	-8.7
<i>G2</i>				
Modified	51.6	-36.3	-30.5	-5.8
Control	45.5	-32.3	-28.2	-4.1

<sup>a</sup> The  $T_M$ s of *Duplex* correspond to a strand concentration of 8  $\mu$ M. Experimental errors are as follows:  $T_M$  ( $\pm 0.5$  °C),  $\Delta H_{cal}$  ( $\pm 5\%$ ),  $T\Delta S$  ( $\pm 5\%$ ) and  $\Delta G$  ( $\pm 7\%$ ).

(G2) and by a favorable differential entropy term for *Triplex*. The enthalpy contributions are explained in terms of stacking contributions, which are associated with the local environment that 2AP is experiencing i.e., strength of base-pair (or base-triplet) stacking and overall hydration state of the nucleic acid molecule. Overall, the incorporation of fluorescent markers in DNA molecules is a useful tool to investigate the conformational flexibility of a nucleic acid structure as a function of temperature. Fluorescence melting curves can monitor the conformational changes, and associated hydration changes, when fluorescent moieties are placed properly in the molecular environment of a nucleic acid. The results will also aid in traditional thermodynamic methods, providing a more sensitive experimental window to follow local changes.

## 5. Acknowledgements

This work was supported by Grants MCB-0616005 and MCB-7111668 from the National Science Foundation. LAM is very pleased to contribute this manuscript to the special issue of Acta Chimica Slovenica dedicated to the retirement of Professor Gorazd Vesnaver. LAM would like to express gratitude to Gorazd for many scientific and non-scientific discussions during his early training (1973–74) as a graduate student at Rutgers University.

## 6. References

- M. K. Shukla, J. Leszczynski, *J. Biomol Struct Dyn.* **2007**, 25, 93–118.
- S. Roy, *Methods in Enzymology* **2003**, 370, 568–576.
- A. K. Shchyolkina, D. N. Kaluzhny, D. J. Arndt-Jovin, T. M. Jovin, V. B. Zhurkin, *Nucleic Acids Research* **2006**, 34, 3239–3245.
- S. P. Parel, C. J. Leumann, *Nucleic Acids Research* **2001**, 29, 2260–2267.
- D. Jose, K. Datta, N. P. Johnson, P. Hv. Hippel, *Proceedings of the National Academy of Sciences of the United States of America* **2009**, 106, 4231–4236.
- D. C. Ward, E. Reich, L. Stryer, *Journal of Biological Chemistry* **1969**, 244, 1228–37.
- T. M. Nordlund, S. Andersson, L. Nilsson, R. Rigler, A. Graeslund, L. W. McLaughlin, *Biochemistry* **1989**, 28, 9095–9103.
- L. C. Sowers, G. V. Fazakerley, R. Eritja, B. E. Kaplan, M. F. Goodman, *Proceedings of the National Academy of Sciences of the United States of America* **1986**, 83, 5434–5438.
- S. M. Law, R. Eritja, M. F. Goodman, K. J. Breslauer, *Biochemistry* **1996**, 35, 12329–12337.
- O. J. G. Somsen, A. Van Hoek, H. Van Amerongen, *Chemical Physics Letters* **2005**, 402, 61–65.
- E. L. Rachofsky, R. Osman, J. B. A. Ross, *Biochemistry* **2001**, 40, 946–956.
- J. M. Jean, K. B. Hall, *Proceedings of the National Academy of Sciences of the United States of America* **2001**, 98, 37–41.
- D-G. Xu, T. M. Nordlund, *Biophysical Journal* **2000**, 78, 1042–1058.
- R. Eritja, B. E. Kaplan, D. Mhaskar, L. C. Sowers, J. Petruska, M. F. Goodman, *Nucleic Acids Research* **1986**, 14, 5869–5884.
- J. T. Stivers, *Nucleic Acids Research* **1998**, 26, 3837–3844.
- K. B. Hall, D. J. Williams, *RNA* **2004**, 10, 34–47.
- T. Kimura, K. Kawai, M. Fujitsuka, T. Majima, *Chemical Communications* **2004**, 12, 1438–1439.

18. K. Evans, D. Xu, Y. Kim, T. M. Nordlund, *Journal of Fluorescence* **1992**, 2, 209–216.
19. R. D. Gray, L. Petraccone, J. O. Trent, J. B. Chaires, *Biochemistry* **2010**, 49, 179–194.
20. J. D. Ballin, S. Bharill, E. J. Fialcowitz-White, I. Gryczynski, Z. Gryczynski, G. M. Wilson, *Biochemistry* **2007**, 46, 13948–13960.
21. N. P. Johnson, W. A. Baase, P. H. Von Hippel, *Proceedings of the National Academy of Sciences of the United States of America* **2004**, 101, 3426–3431.
22. R. K. Neely, D. Dajutyte, S. Grazulis, S. W. Magennis, D. T. F. Dryden, S. Klimauskas, A. C. Jones, *Nucleic Acids Research* **2005**, 33, 6953–6960.
23. Y. Takeda, P. D. Ross, C. P. Mudd, *Proceedings of the National Academy of Sciences of the United States of America* **1992**, 89, 8180–8184.
24. T. Kimura, K. Kawai, M. Fujitsuka, T. Majima, *Tetrahedron* **2007**, 63, 3585–3590.
25. C. M. Olsen, H-T. Lee, L. A. Marky, *J. Phys. Chem. B* **2009**, 113, 2587–2595.
26. C. M. Olsen, W. H. Gmeiner, L. A. Marky, *J. Phys. Chem. B* **2006**, 110, 6962–6969.
27. X. Mao, L. A. Marky, W. H. Gmeiner, *J. Biom. Struc. & Dyn.* **2004**, 22, 1–9.
28. L. A. Marky, K. J. Breslauer, *Biopolymers* **1987**, 26, 1601–1620.
29. H-T. Lee, S. Arciniegas, L. A. Marky, *J. of Phys. Chem.* **2008**, 112, 4833–4840.
30. H-T. Lee, I. Khutsishvili, L. A. Marky, *Journal of Physical Chemistry B* **2010**, 114, 541–548.
31. M. Kawai, M. J. Lee, K. O. Evans, T. M. Nordlund, *Journal of Fluorescence* **2001**, 1, 23–32.
32. T. M. Nordlund, *Photochemistry and Photobiology* **2007**, 83, 625–636.
33. R. Shikiya, L. A. Marky, *J. Phys. Chem. B* **2005**, 109, 18177–18183.
34. A. M. Soto, J. Loo, L. A. Marky, *J. Am. Chem. Soc.* **2002**, 124, 14355–14363.
35. A. M. Soto, D. Rentzeperis, R. Shikiya, M. Alonso, L. A. Marky, *Biochemistry* **2006**, 45, 3051–3059.
36. C. M. Olsen, L. A. Marky, *Journal of Physical Chemistry B* **2009**, 113:9–11.

## Povzetek

Fluorescenčni označevalec 2-aminopurin (2AP) pogosto uporabljamo za spremljanje okolja, v katerem se nahajajo molekule nukleinskih kislin (n. k.) in ligandov, ki se nanje vežejo. To vključuje lokalno okolico s topilom in celokupno dinamiko n. k. in njihovih kompleksov z ligandi. Naše delo poroča o spremembi konformacijske fleksibilnosti različnih sekundarnih struktur n. k. v odvisnosti od temperature. Za spremljanje konformacijskih sprememb ob višanju temperature (t.i. taljenje, razvitje oz. denaturacija) smo uporabili spektroskopske in kalorimetrične tehnike. Raziskali smo uporabnost merjenja fluorescence 2AP pri spremljanju »taljenja« n. k. in prvič tudi sposobnost nalaganja (»stacking«) 2AP v različnih strukturah n. k. Podrobno smo proučili vpliv substitucije A → 2AP na stabilnost različnih struktur DNA kot so enoverižna (SS), dodekamerna dvoverižna (Duplex), t. i. lasnica (Hairpin), G-kvadrupleks (G2) in tripleks tvorjen iz ene verige DNA (Triplex). Fluorescenčna, UV absorpcijska in CD spektroskopija ter diferenčna dinamična kalorimetrija (DSC) so bile uporabljene pri spremljanju razvitja teh struktur ob višanju temperature. Vse omenjene metode dajo za vsako od izbranih DNA »monofazne« talilne krivulje, ki rezultirajo v podobnih talilnih temperaturah ( $T_M$ ) in van't Hoff-ovih entalpijah razvitja, kar kaže na to, da je v primerih vseh DNA razvitje prehod med dvema stanjema in da spremembe fluorescence ob spremembi okolja 2AP (»unstacking«) odražajo razvitje celotne molekule DNA. Na osnovi DSC dobljeni termodinamski profili zvitja za modificirane DNA (A → 2AP) relativno glede na njihove nemodificirane oblike kažejo naslednje vrednosti  $\Delta\Delta G^\circ$ : 1.6 kcal/mol (Duplex), 3.1 kcal/mol (Hairpin), 1.6 kcal/mol (Triplex) in -1.7 kcal/mol (G2). Te so odraz neugodne diferenčne entalpije (Duplex in Hairpin), ugodne diferenčne entalpije (G2) in ugodnega prispevka diferenčne entropije za Triplex. Entalpijske vplive lahko razložimo s prispevkoma »stackinga« in hidratacije, ki sta povezana z lokalnim okoljem, ki ga zaznava 2AP. Na primer za 8.7 kcal/mol nižja vrednost  $\Delta\Delta H_{cal}$  za Hairpin glede na Duplex je odraz šibkejšega nalaganja (»stacking«) baznih parov in močnejše hidratacije v korenu molekule Hairpin-a. Zaključimo lahko, da je vključitev 2AP v n. k. uporabna za spremljanje njihove toplotne denaturacije, še posebej kadar je ta fluorescenčni označevalec umeščen v ustrezno okolje v n. k.